Successful Betatron Acceleration of Kiloampere Electron Rings in RECE-Christa

D. P. Taggart, M. R. Parker, H. J. Hopman,
R. Jayakumar, and H. H. Fleischmann
School of Applied and Engineering Physics, Cornell University, Ithaca, New York 14853
(Received 19 December 1983)

This paper reports on betatron acceleration experiments using the space-charge-neutralized electron rings in the RECE-Christa device. Magnetic-probe and x-ray-absorption measurements indicate that electron ring currents of up to 2 kA were accelerated to 3.3 ± 0.3 MeV without indication of instabilities. A similar neutralization and acceleration method also appears applicable to electron rings generated in B_θ-free configurations.

PACS numbers: 29.20.Fj, 52.75.Di

Since Kerst's original success,[4] betatron accelerators have been used for the production of megaelectronvolt electrons. Various modifications were conceived and investigated with the goal of increasing the maximum ring current. In the conventional betatron, the ring current is limited to below ampere strength[2] because of space-charge problems during injection. In later designs[3] this limit was raised to about 90 A by use of higher injection energies E_0 of up to several hundred kiloelectronvolts. Following the original proposal of Sprangle and Kapetanakos,[4] increasing interest presently focuses on "modified betatron" arrangements in which the space-charge effects are reduced by adding a strong toroidal field; in this area, the experiment[5] at the University of California at Irvine so far has obtained an energy-integrated current of about 150 A, and the larger experiment at the Naval Research Laboratory,[6] presently under construction, expects to obtain 5 kA of 50-MeV electrons. As a separate path, Budker[7] proposed to avoid the space-charge problem altogether in a "plasma betatron" by acceleration of runaway electrons from a preformed plasma. Corresponding experiments, however, seemed to be limited by plasma instabilities, with ring currents and energies claimed[8] for such devices ranging up to 100 A and 2 MeV, respectively. A similar runaway-electron situation also has occurred in various tokamak experiments: In some of these,[9] fast-electron currents of up to ~ 200 A (i.e., a small fraction of the total discharge current) have been reported for energies ~ 10 MeV; in other high-current "beam" discharges, runaway-electron currents of about 65 kA with a very broad energy spectrum (due to beam-plasma instabilities and continuous runaway-electron generation) were obtained by adding high-Z gases,[10] or the electron energies were limited to around 100 keV.[11]

The present paper describes experiments in which strong space-charge–neutralized electron rings trapped in the RECE-Christa device (RECE denotes relativistic electron coil experiment) are accelerated in a betatron arrangement. As in the earlier Astron[12] experiment, the rings are generated through tangential injection of fast electrons in combined axial and toroidal fields with, however, the toroidal fields quite small compared with those to be used in the modified betatron scheme or in runaway-electron tokamak discharges. In contrast to the normal plasma-betatron experiments, our electron rings (initially about 1 MeV) exist in a cold and only partially ionized hydrogen plasma which is less prone to instabilities. The arrangement is also similar to the Astron-type experiment at Irvine[13] in which injected lower-energy electrons are trapped and accelerated, with a total ring current of up to 10 A so far being accelerated to energies of about 1 MeV.

In our experiments, so far, electron rings with final ring current of 2 kA were accelerated to energies of 3.3 MeV without indications of instability.

The RECE-Christa device, used in our experiments, is described in more detail elsewhere.[14] In brief, an intense electron beam pulse (typically 2 MeV peak, 40 kA, 80 nsec) is azimuthally injected into a magnetic field consisting of an axial mirror field $B_z = 400$–500 G, a toroidal field B_θ generated by an axial current $I_z = 50$–110 kA, and the fields due to various pulsed coils. The rings initially are trapped upstream in a puffed-in gas cloud and then moved axially into the low-density magnetic-well region downstream. In the present experiments the arrangement shown in Fig. 1 is used downstream. The magnetic well is positioned within the compression coil used earlier.[15] When energized from another capacitor bank ($t_{1/4} = 260$ μsec), this coil raises the axial field by $B_c < 2$ kG. In addition, an accelerator coil (10 cm in diameter, 1.5 m long, 180 windings) is placed along the tank axis. When energized from another capacitor bank ($t_{1/4} = 270$ μsec, $V_{max} = 6$ kV) this coil will induce a toroidal field E_θ that accelerates the electrons in the ring.

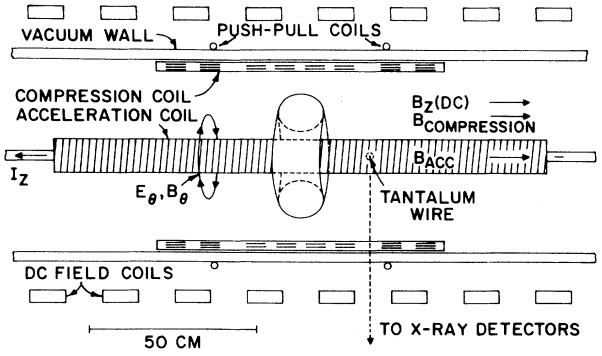

FIG. 1. The accelerator arrangement.

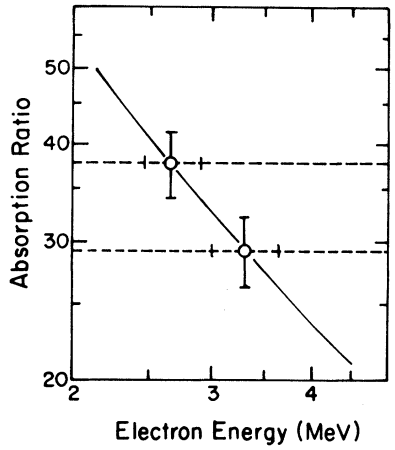

FIG. 2. Energy dependence of the predicted absorption ratio, and measured (circles) absorption ratios.

The relative strength of the compression and acceleration fields can be adjusted for control of the ring radius during the acceleration. In addition to the normal gas puff upstream, a steady-state gas fill of 50–100 mTorr is used in the tank, producing a highly collisional background plasma in the ring with $n_p \approx 10^{11}$–10^{12} cm^{-3} and $T_e < 1$–2 eV.[16]

The magnetic ring parameters are diagnosed with use of a set of $\dot{B}$ probes positioned along the tank axis and the wall. All probe responses are integrated passively ($RC = 2$–10 msec), and digitally recorded and analyzed. The relevant ring parameters (ring current and geometry) are derived from the probe signals after subtraction of all baseline fields by use of our normal procedures.[16]

The energy of the accelerated electrons is determined through x-ray absorption spectroscopy. A Ta wire (1 mm diameter) is stretched vertically between the center conductor and the compression coil 20 cm downstream from the magnetic well. After acceleration, the rings are brought into contact with the wire by activating a set of push-pull coils that move the ring downstream. The forward-directed x rays generated by the fast electrons in the wire are observed by two well-shielded NaI detectors (5-in.$\times$5-in. and 2-in.$\times$2-in., respectively). The collimated viewing area of the larger detector "sees" the wire from the center conductor to a radius of 23 cm, i.e., within 4 cm of the compression coil. The viewing area of the 2-in.$\times$2-in. detector is somewhat wider, including the full wire length. The detector signals are RC integrated with $RC = 50$ μsec. Normally, the entrance channels of both detectors are covered with 5 cm of lead, absorbing essentially all x rays below about 500 keV. Absorption measurements then are performed by alternately placing and removing a 10-cm Fe absorber into and out of the entrance channel of the 5-in.$\times$5-in. detector while using identical acceleration conditions. In this, the signal of the smaller detector is used as an x-ray monitor for normalization in order to reduce shot-to-shot fluctuations resulting from variations in ring parameters (ring current and radius, final energy, etc.). The absolute intensity of the larger detector has been calibrated with use of the line radiation of a ^{22}Na source.

The average beam energy is obtained by comparing the measured Fe absorption ratios with Monte Carlo–calculated ratios. In deriving the latter, the forward-directed bremsstrahlung spectrum for a monoenergetic (energy E_0) and parallel electron beam hitting the wire has been approximated by using the thick-target data of Dickinson and Lent[17] and Halbleib.[17] Using this spectrum, we calculated the response of the larger detector with and without the Fe absorber for $E_0 = 2$, 3, and 4 MeV using the Los Alamos Scientific Laboratory Monte Carlo code[18] MNCP with the full existing tank and absorber geometry. The resulting energy dependence of the predicted absorption ratio is shown in Fig. 2. In this, the interpolation between the calculated points was done by comparison with curves calculated from total interaction cross sections, with the absolute differences between the latter and the Monte Carlo points being of order 10%.

Obviously, some uncertainties exist in this calculation even for monoenergetic electrons. Considering the multiple scattering and the slowdown of the fast electrons in the wire, it is clear that the accelerated electrons will not be stopped in the wire in all cases. However, the related changes in the x-ray spectrum will occur mainly in the low-energy range which is essentially cut off by the lead absorbers. Remaining changes at the high-energy end would

appear mainly in a reduction (estimated as 10%–20%) of the overall intensity. Deviations of the impact angle of the fast electrons on the wire (from the exact θ direction) may occur from the angular spread of the fast electrons in the ring as well as from inhomogeneities in the external field. Looking at the data of Ref. 17 and related details, we estimate that such angular deviations would influence the absorption ratios only by a few percent (upward, i.e., towards larger apparent beam energies) even for an average spread of 20–30 deg; the absolute signal intensities, however, may be decreased in this case already quite significantly (up to a factor 2–3). However, these uncertanties are sizably larger for the initial ring parameters so that the method cannot be used for that case.

Figure 3 shows a typical set of recordings. Part (a) shows the ring-generated field as recorded by a set of axial probes downstream (after correction for base fields and integrator errors). The ring (field reversal $\sim 50\%$) is seen initially entering the accelerator region and settling between probes 19 and 20. At the start of the acceleration phase, the ring recenters and the ring-generated fields increase somewhat. Thereafter, the ring fields decay smoothly and without indication of gross instability. At completion of the acceleration phase, the ring moves further downstream into the Ta target. Part (b) shows the derived ring radius after a small initial increase (due to a small timing difference between the acceleration and compression fields); this radius remains constant within an overall uncertainty of about 5%. Part (c) shows the derived total ring current. Its initial increase appears to be due to a toroidal acceleration and alignment of the fast electrons and also some cross-field plasma currents (probably 200–300 A) as well as some signal perturbation resulting from changes of the coil currents due to the ring. Finally, the x-ray detector signals [Fig. 3(d)] indicate some fast-electron losses (at lower energies) already during acceleration and then a large burst when the ring is moved into the target.

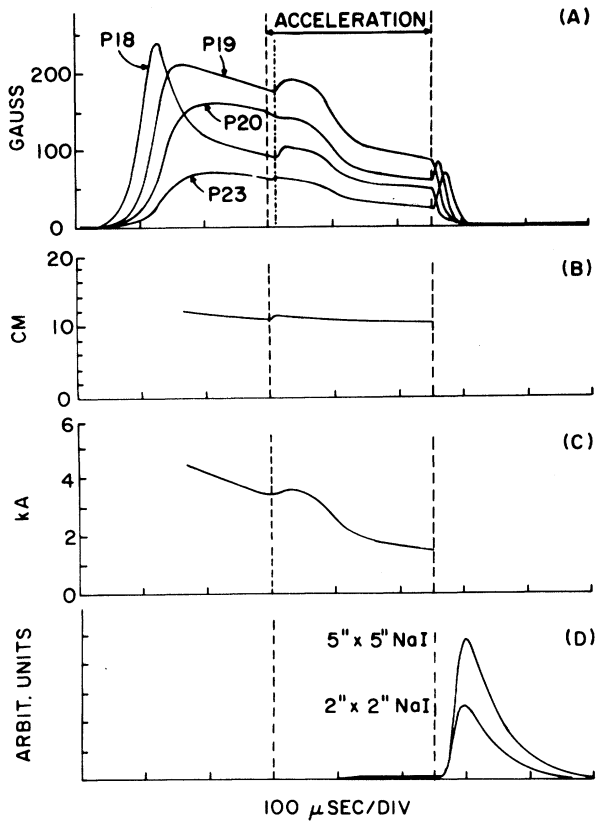

FIG. 3. Typical shot recordings: (a) ring-generated fields at various probes, (b),(c) derived ring radius and current, and (d) x-ray detector signals. (Dot-dashed line indicates 15-μsec delay between firing of compression and acceleration coils.)

With use of identical machine conditions, recordings were taken for eleven shots with and without the Fe absorber. From these data, an absorption ratio of 29 ± 3 was derived for the Fe absorber (the error limit is derived from a 10% rms fluctuation of the normalized response of the 2-in.$\times$2-in. detector and the rms fluctuation of the signal ratios of the two detectors of 10% and 15% without and with the Fe absorber, respectively). With use of a smaller acceleration, $V_{acc} = 4$ kV, an absorption ratio of 38 ± 4 was observed. Both of these results are compared with the calculated ratios in Fig. 2, yielding final beam energies of 3.3 ± 0.3 MeV and 2.6 ± 0.3 MeV for $V_{acc} = 6$ and 4 kV, respectively.

Considering overall experimental uncertainties of about 10%, the inferred final energy of 3.3 MeV for $V_{acc} = 6$ kV is quite consistent with the measured ring radius of 10.5 cm and the final axial field of 1180 G. Assuming an initial beam energy of 1.1 MeV (as indicated by initial ring radius and axial field) and an electron velocity purely in the θ direction, we calculate an expected final energy of 4.1 MeV using the existing field changes and the collisional energy losses in the 50-mTorr gas fill. While somewhat higher, this value becomes quite consistent with the observed value when consideration is given to the effects of the initial angular spread of the beam, making $V_\theta < c$, and of the sizable pressure increase due to the precursor of the expanding gas cloud.

A similar situation exists regarding the observed absolute x-ray intensity. Although the measured

intensity is low by about 50% relative to the simple forward-directed thick-target value for 3.3 MeV, the intensity loss expected for a wire target together with an average angular deviation of the impinging electrons of only 15°–20° are sufficient for reconciling the two intensities. A similar situation also applies to the case with $V_{acc}=4$ kV.

In summary, the observed final energies and intensities are in good agreement with those expected for the experiment. Interesting, and not fully explained yet, is the 50% loss in beam strength during acceleration. At least in part, it may be due to a reduction of the external mirror ratio by the return flux of the acceleration coil. However, it may be related also to the energy homogenization and radial thinning of the ring to be expected from the near $1/r$ dependence of E_θ; a partial Φ_θ conservation will then tend to make the ring spread in axial direction. Either explanation may explain x-ray emission from the wire observed during acceleration. More detailed investigations on this point will be needed.

Obviously, the employed beam neutralization and acceleration also may be applied to rings without B_θ as were generated in some of our earlier experiments.[19,20] Related experiments are in progress.

Finally, we would like to express our sincere appreciation to C. E. Swannack and R. G. Schrandt for providing us with the Monte Carlo program and for help in its execution, and to J. Milks for his unceasing and valuable technical assistance during the experiments.

[1]D. W. Kerst, Phys. Rev. **58**, 841 (1940).

[2]D. W. Kerst *et al.*, Phys. Rev. **78**, 297 (1950).

[3]A. I. Pavlovskii *et al.*, Dokl. Akad. Nauk SSSR **160**, 68 (1965) [Sov. Phys. Dokl. **10**, 30 (1965)].

[4]P. Sprangle and C. A. Kapetanakos, J. Appl. Phys. **49**, 1 (1978).

[5]H. Ishizuka *et al.*, Bull. Am. Phys. Soc. **28**, 1039 (1983).

[6]C. A. Kapetanakos *et al.*, Phys. Fluids **26**, 1634 (1983).

[7]G. J. Budker, in *Proceedings of the CERN Symposium on High-Energy Accelerators and Pion Physics, Geneva, 1956* (CERN Scientific Information Service, Geneva, 1956), Vol. 1, pp. 68,76.

[8]For example, J. G. Linhart, in *Proceedings of the Fourth International Conference on Ionization Phenomena in Gases, Uppsala, Sweden, 1959,* edited by N. Robert Nilsson (North-Holland, Amsterdam, 1960), p. 981.

[9]H. Knoepfel and S. J. Zweben, Phys. Rev. Lett. **35**, 1340 (1975).

[10]H. Knoepfel, D. A. Spong, and S. J. Zweben, Phys. Fluids **20**, 511 (1977).

[11]G. Fussman *et al.*, Phys. Rev. Lett. **47**, 1004 (1981).

[12]R. J. Briggs *et al.*, Phys. Fluids **16**, 1934 (1973).

[13]R. Prohaska *et al.*, Bull. Am. Phys. Soc. **28**, 1038 (1983).

[14]H. A. Davis *et al.*, Phys. Rev. Lett. **37**, 542 (1976).

[15]M. Tuszewski *et al.*, Phys. Rev. Lett. **43**, 449 (1979).

[16]D. J. Rej, M. R. Parker, and H. H. Fleischmann, Phys. Fluids **26**, 323 (1983).

[17]W. Dickinson and E. Lent, University of California Report No. UCRL-50442, 1968 (unpublished); J. A. Halbleib, Sandia Laboratory Report No. SC-RR-72 0435, 1972 (unpublished).

[18]Los Alamos Monte Carlo Group, Los Alamos Scientific Laboratory Report No. LA-7396-M, Revised, 1981 (unpublished).

[19]J. J. Bzura *et al.*, Phys. Rev. Lett. **29**, 256 (1972).

[20]R. E. Kribel *et al.*, Plasma Phys. **16**, 113 (1974).